COBALT-PLATINUM (CoPt) MIXED SUBNANOPARTICLES WITH THE INTERACTION OF ETHYNYL ANION (C_2H^-): A DFT MATERIAL MODELING STUDY

Mikail ASLAN[1,*]

[1]*Department of Metallurgical and Materials Engineering, Faculty of Engineering, Gaziantep University, Gaziantep, Turkey*

ABSTRACT

The purpose of most of the computational material science studies is to determine the relationship between structure and property alteration. The knowledge of the property variation with geometry also allows one to carry out material computer experiments to design new stable nanoparticles with desired properties. The DFT study carried out in the present work on the small bimetallic anionic Co_nPt_m-ethynyl nanoparticles reveals that Pt content in the lowest energetic nanoparticles lead to increase in chemical stability of the structures that play significant role in nanoparticles for preserving current condition. The highest HLG belongs to $[Pt_3C_2H]^-$ which indicates their chemical stability. Furthermore, the vibrational frequency calculations will guide future spectroscopic experiments.

Keywords: DFT, Organometallic Nanoparticles, Subnanoalloys, Computational Material Science Engineering, Ethynyl Molecules.

1. INTRODUCTION

Computational methods are widely used tools for the fields of chemistry, physics, and material science engineering. The increasing speed and availability of computational resources in grouping with newly developed and increasingly accurate models provides scientists and engineers to solve and rationalize chemical phenomenon. The purpose of most of the computational material science studies is to determine the relationship between structure and property alteration. The knowledge of the property variation with geometry also allows one to carry out material computer experiments to design new stable NPs with desired properties. Additionally, computer simulations allow us to investigate probabilities to check whether the exciting properties of nanoparticles (NPs) are preserved in different environments. For instance, it can be determined whether the high magnetic moments of gas-phase NPs will be retained when they are deposited on a substrate. It also allows one to check whether highly stable NPs can be assembled to form solids. This type of approach can lead us to the development of novel NPs based materials. Another point is that the experiments on NPs especially on gas-phase NPs yield little information about their structures. In this regards, simulations complement the experiments by providing structural input. From the application point of view, the interaction between NPs and substrate matrix is of paramount importance. The properties of such systems are governed by many body electron ion interactions.

In recent years, a great deal of effort for studying magnetic CoPt nanoalloy clusters [1-29] has been shown by engineers and scientists due to their potential usage in ultra-high density magnetic storage applications [30]. The characterization of the magnetic anisotropy energy distribution of a diluted assembly of CoPt NPs with a mean diameter of 3 nm by using superconducting interference device magnetometry was reported by Tournus et al. They found experimental evidence of a magnetic anisotropy constant dispersion with a comparison of unselected CoPt clusters and size-selected Co clusters [31]. Tizitzios et al. reported the production of 3D ferromagnetic CoPt nanostructures [14]. A theoretical study was conducted by Feng et al. [32]. They examined magnetic and electronic properties of CoPt NPs having equal number of Pt and Co atoms.

Using ligand functional groups adsorbed metal atoms surface allows binding NPs and the construction of functional nanoassemblies to various substrates surfaces. Besides, ligand environment affects the electronic properties of the clusters. There is huge amount of studies available for subnanoalloy or pure metal NPs but much less computational emphasis has been devoted to the ligation of these NPs. This computational study may be a contribution to the understanding of the role of ligands on the stabilization of metal NPs to design new stable structures with desired properties. Consequently, Investigation of CoPtC2H metalorganic subnanoalloys will be worthy to identify the mechanism and find more details on the formation of these NPs.

2. METHODOLOGY

The low energetic local stable isomers are calculated by NWChem 6.0 soft*ware* [33] within the framework of Density Functional Theory (DFT). Furthermore, we have calculated total energies, vibration frequencies, and HOMO-LUMO energy gaps (HLG). In order to reduce the number of electrons in the computation, which reduces time cost, for Pt and Co elements, CRENBL [34] basis set and relativistic effective core potential (ECP) have been used while for

C and H atoms, the split valence 6-31G* basis set has been used. The reliability of the basis sets were checked by the reference [34]. $1\text{x}10^{-6}$ Hartree for energy and $5\text{x}10^{-4}$ Hartree / a_0 for energy gradient have been employed in the calculations. Becke's 1988 exchange functional [35] and Lee-Yang-Parr correlational functional [36] have been used. The structures are relaxed without any geometric constraints in various magnetic moments.

3. RESULT AND DISCUSSION

The lowest energetic structures of $[Co_xPt_yC_2H]^{-1}$ ($2 \leq x+y \leq 3$) NPs are given in Figure 1, considering various spin multiplicities and initial configurations. Furthermore, in Table 1, spin moments, binding energies per atom (BE), HLGs, vertical detachment energies (VDE) and range of vibrational frequencies of the NPs are listed.

Table 1 The electronic properties of Co_xPt_y-ethynyl clusters

Clusters		**Spin moment (μ_B)**	**BE per atom (eV)**	**HOMO-LUMO Gap (eV)**	**VDE (eV)**	**Lowest and Highest Vibrational Frequencies (cm^{-1})**
$[Co_2C_2H]^-$	Present Work	4	4.46	0.33	1.25	55-3360
	Literature				1.53*	
	Exp.				1.50*	
$[CoPtC_2H]^-$		3	5.08	0.63	2.53	37 -3369
$[Pt_2C_2H]^-$		2	5.26	0.28	2.66	43-3384
$[Co_3C_2H]^-$	Present Work	7	4.29	0.03	1.52	64-3368
	Literature				1.59*	
	Exp.				1.81*	
$[Co_2PtC_2H]^-$		4	4.71	0.73	1.47	68-3154
$[CoPt_2C_2H]^-$		3	4.89	0.72	2.26	56-3387
$[Pt_3C_2H]^-$		0	5.06	1.05	1.64	41- 2968

*[8]

3.1 $[Co_xPt_yC_2H]^{-1}$ (x+y=2)

Some of the low-lying isomers of anionic Co_xPt_y-ethynyl (x+y=2) clusters are displayed in Figure 1. The C-C bond distance of the free ethynyl molecule is calculated as 1.25 Å. The obtained results show that when the molecule is adsorbed on an atop side, this bond length is not changed so much.

The lowest energetic structure of $[Co_2C_2H]^{-1}$ NPs is identified as a linear structure with C_s symmetry. When C_2H molecule approaches to Co dimer, the C atom at the end of the molecule binds to the Co atom. In this structure the Co-C bond distance is 1.92 Å, the Co-Co bond distance is 2.38 Å and the magnetic state is the quintet state (4 μ_B spin moment). The Co-Co bond distance of pure diatomic cobalt particle is given between 1.99 Å and 2.13 Å in the literature. These calculated values of bond lengths are in good agreement with the previous theoretical calculations of the Co-Co bond length as 2.43 Å and the Co-C bond length as 1.95

Å [8]. The BE and VDE of this structure are calculated as 4.46 eV and 1.25 eV (see Table 1). The magnetic moment of 1C is 6 μ_B while 1A and 1B are 4 μ_B and 1B has a relative energy of 0.91 eV with respect to the lowest energy structure 1A.

The ground state configuration of $[CoPtC_2H]^{-1}$ is a linear structure with C_s group symmetry. The C_2H is adsorbed onto the Co atom rather than the Pt atom where the C-Pt bond distance is 2.28 Å. The elongation between Co-Pt distance upon ethynyl molecule absorption is by 0.04 Å while the Co-Pt bond length in pure bimetallic CoPt nanoalloy is 2.24 Å. The second low-lying minima of $[CoPtC_2H]^{-1}$ is also a linear structure, which has 0.59 eV higher energy than the lowest one. The magnetic moments of 2A and 2B are 3 and 1 μ_B respectively and the third isomer 2C has 3 μ_B , which has 0.78 eV higher energy than the ground state. The ground state configuration of the anionic Pt dimer-ethynyl cluster with C_s symmetry is nonlinear planer structure in the triplet magnetic state. The angle between Pt-Pt-C atoms is 160°. The Pt-Pt distance in the pure Pt dimer is 2.21 Å. The adsorption of ethynyl molecule leads to a stretch in the Pt-Pt bond length where the Pt-Pt bond distance becomes 2.46 Å. In addition, bridge site adsorptions have higher energy than atop site adsorption, which continues for the trend that atop site adsorption has lower energy than bridge site adsorption. The elongation for Pt-Pt and C-C distance is by 0.24 Å and 0.05 Å respectively in bridge site adsorption whereas there is no significant change for the typical Pt-C distance in both adsorption types.

3.2 $[Co_xPt_yC_2H]^{-1}$ (x+y=3)

The VDE of the particles for x+y=3 ranges from 4.29 to 5.06 eV (see Table 1). The doping of the Pt atom in these structures leads to increase in VDE. Furthermore, the C-C bond distance in ethynyl molecule in the lowest ground state isomers is between 1.24 and 1.44 Å where the C≡C bond of acetylene (1.20 Å) [37] and the C=C bond of ethene (1.33 A) [38].

Different research groups calculated the lowest energy structure of bare cobalt trimer and reported a triangular structure and a linear structure [39-43]. Yoshida et al. reported Co-Co distances of the anionic bare Co trimer in the linear structure between 2.25-2.50 Å in their experimental and theoretical calculations [44]. The lowest energy structure (4A) of the anionic Co_3-ethynyl nanoparticle is a planar Y-like structure with a BE of 4.29 eV and it has high point group symmetry, C_{2v} with 7 μ_B spin moment. The average Co-Co bond distance in this ground state structure, which has a perfect isosceles triangular Co_3 unit, is 2.4 Å. Furthermore, the addition of one Co atom to the $[Co_2C_2H]^-$ leads to increase in VDE where the VDE in the structure 4A is 1.52 eV that is consistent with the results in Ref [8] (see Table 1). The second isomer 4B and the third isomer 4C have approximately the same relative energies with respect to the ground state energy although they are in different magnetic states. The forth isomer 4D is constructed by the bridge side binding of the terminal C atom of the ethynyl molecule, which is in the octet magnetic state. The Co-C bond lengths are 2.04 and 1.96 Å in this structure.

As a Co atom is changed with a Pt atom in the structure, the ground state of anionic Co_2Pt-ethynyl NP becomes the structure of a triangular bimetallic unit including a Pt atom at the apex and two Co atoms at the base with average Co-Pt bond length of 2.44 Å. While the distances between Co and Pt atoms are stretched slightly as the amounts of 0.06 and 0.11 Å, the separation between Co atoms is shrunk as much as 0.15 Å after the adsorption of ethynyl molecule. Its BE is 4.71 eV/atom where the quintet magnetic state is the same with the bare Co_2Pt cluster. In the second isomer 5B where ethynyl molecule binds atop site, the Co-C bond distance is 1.92 Å with a relative energy of 0.49 eV with respect to the lowest energy structure. The third isomer 5C and the forth isomer 5D have average Co-C bond lengths of 1.91 Å and 1.98 Å, respectively.

As Pt doping increases, the BE of anionic $CoPt_2$-ethynyl increases to 4.89 eV. For this species (6A), ethynyl molecule prefers energetically to bind Pt atom rather than Co atoms, which is different from the bridge side adsorption of the previous case.

The BE of anionic Pt_3-etynyl cluster is calculated as 5.06 eV which is the highest value for x+y=3 systems. According to the calculations, doping of Pt atom to the NPs lead to increase in BE value. However, the difference in the BE of $[CoPt_2C_2H]^{-1}$ and $[Pt_3C_2H]^{-1}$ (0.17 eV) is close to that of $[Co_2PtC_2H]^{-1}$ and $[CoPt_2C_2H]^{-1}$ (0.18 eV) while it is smaller than that of $[Co_3C_2H]^{-1}$ and $[Co_2PtC_2H]^{-1}$ (0.42 eV). In this structure, four coordination of Carbon that indicates sp^3 hybridization resulting from delocalized electrons in ethynyl molecule was seen for the first time among all nanoparticles we have mentioned so far. This triggers to expand the C-C bond length in C_2H molecule importantly. In addition, the second isomer 7B has the same singlet magnetic moment as the case of the isomer 7A (see Figure 1) while the magnetic state of the third isomer 7C is triplet.

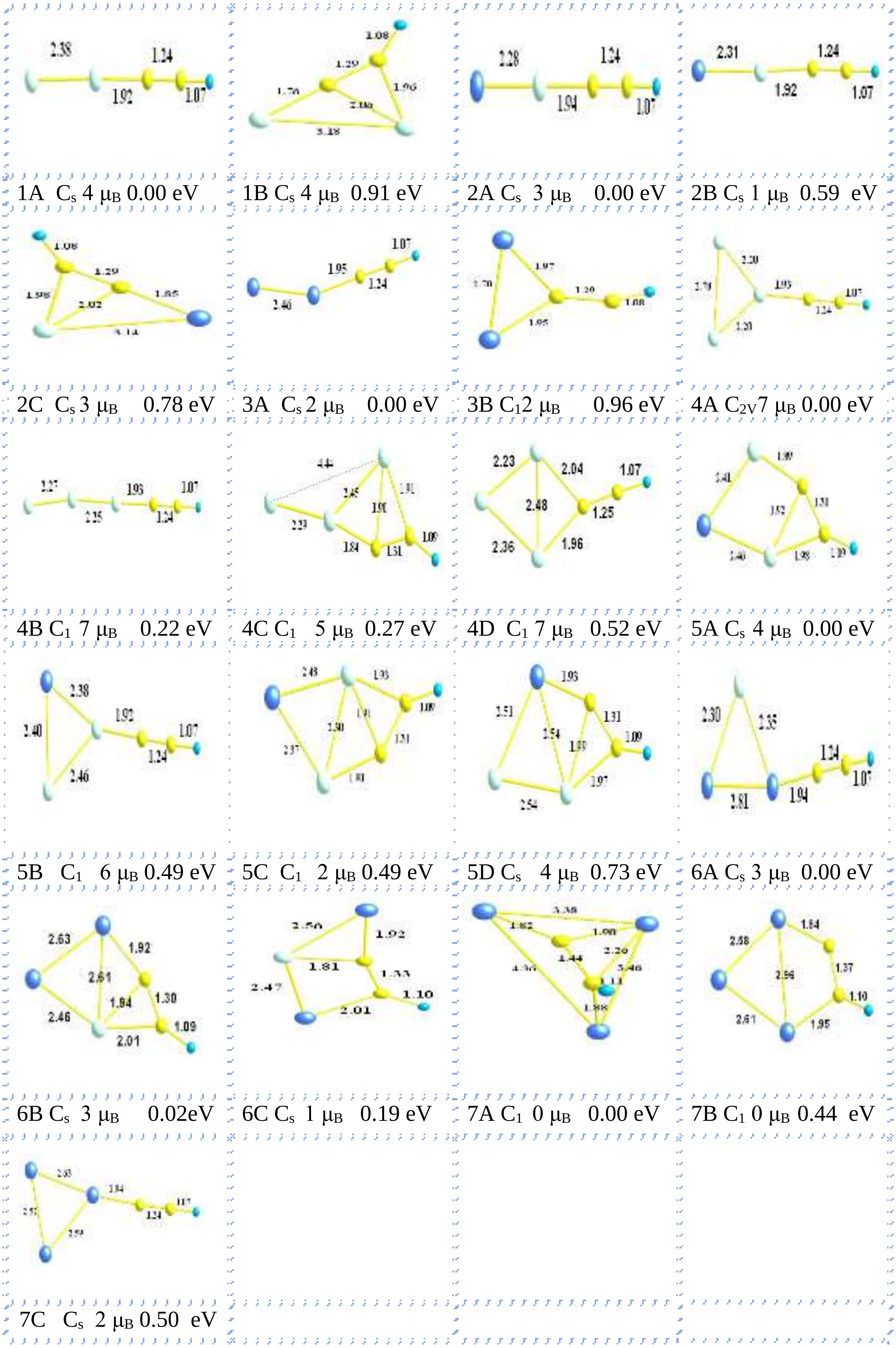

1A C_s 4 μ_B 0.00 eV

1B C_s 4 μ_B 0.91 eV

2A C_s 3 μ_B 0.00 eV

2B C_s 1 μ_B 0.59 eV

2C C_s 3 μ_B 0.78 eV

3A C_s 2 μ_B 0.00 eV

3B $C_1$2 μ_B 0.96 eV

4A C_{2V}7 μ_B 0.00 eV

4B C_1 7 μ_B 0.22 eV

4C C_1 5 μ_B 0.27 eV

4D C_1 7 μ_B 0.52 eV

5A C_s 4 μ_B 0.00 eV

5B C_1 6 μ_B 0.49 eV

5C C_1 2 μ_B 0.49 eV

5D C_s 4 μ_B 0.73 eV

6A C_s 3 μ_B 0.00 eV

6B C_s 3 μ_B 0.02eV

6C C_s 1 μ_B 0.19 eV

7A C_1 0 μ_B 0.00 eV

7B C_1 0 μ_B 0.44 eV

7C C_s 2 μ_B 0.50 eV

Figure 1 The optimized structures of some isomers of $[Co_xPt_yC_2H]^{-1}$ $(2\leq x+y\leq 3)$

3.5 Energetic Calculations

To calculate the binding strength of the studied NPs, the BE ranging from 4.29 eV to 5.06 eV are given in Table 1 and shown in Figure 4. The BE is calculated in the following way:

$$BE = \frac{E[H] + 2E[C] + xE[Co] + yE[Pt] - E[Co_x Pt_y C_2 H]^-}{x + y + 3} \tag{1}$$

where $E[*]$ is the lowest energetic structure of energy of H, C, Co, and Pt atoms and the NPs respectively. The lowest BE of the NPs is $[Co_3C_2H]^-$ while the highest BE of the structures is anionic Pt_2-ethynyl. Alloying Co with Pt increases the binding strength of the structures.

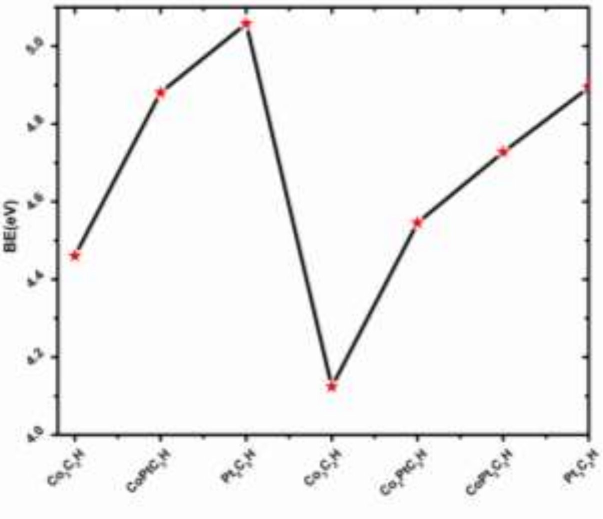

Figure 2 The BE per atom of $[Co_xPt_yC_2H]^-$ for $2 \leq x+y \leq 3$

In terms of the stability of the NPs, second finite difference in energies (D), which is a measure of the relative stability of clusters are calculated as

$$D = E_{x+1,y-1} + E_{x-1,y+1} - 2E_{x,y} \tag{2}$$

Here, $E_{x,y}$ is the lowest energies of studied clusters. D are given in Figure 3. We have found $[Co_2PtC_2H]^{-1}$ NP is more stable when compared the neighboring NPs.

To understand the adsorption ability between Co-Pt species and ethynyl molecule, adsorption energies (E_{ads}) of $[Co_xPt_yC_2H]^{-1}$ nanoalloys are calculated as

$$E_{ads} = E[Co_x Pt_y] + E[C_2 H^{-1}] - E[Co_x Pt_y C_2 H^{-1}] \tag{3}$$

Here, E[*] is the lowest energies of given structures. E_{ads} show a decreasing behavior with the increasing ratio of Co/Pt for the studied species. The trend has no exception for the species having dimer and tetramer metallic units. The adsorption energy of $[Co_2C_2H]^-$ cluster corresponds to a dip (see Figure 3).

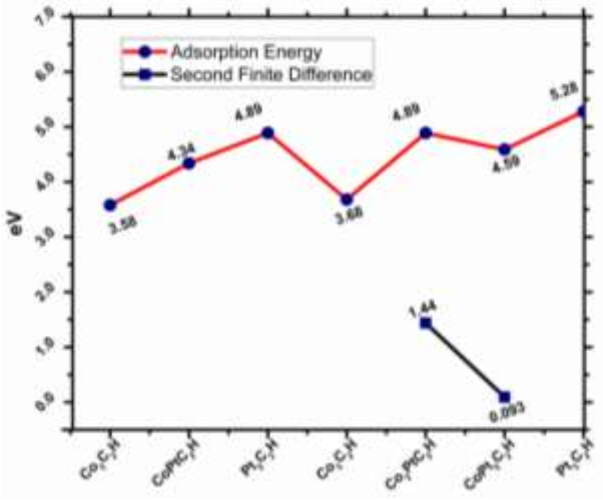

Figure 3 The second finite energies and C_2H^- adsorption energies of $[Co_xPt_yC_2H]^-$

Dissociation energy (E_{dis}) is another sensitive quantity of reflecting relative stability. Within studied range, we have calculated dissociation energies:

$$E_{dis} = E[Co_{x-a}Pt_{y-b}C_2H^-] + E[Co_aPt_b] - E[Co_aPt_bC_2H^-] \quad (4)$$

Dissociation channels and E_{dis} are listed in Table 2. The minimum dissociation energies refer to the most favorable dissociation channel. It can be inferred that the dissociation energy of Pt is larger than that of Co. This is consistent with the trend seen in the BEs. Furthermore, the most favorable reactions are

$Co_3C_2H^- \rightarrow Co_2C_2H^- + Co$
$Co_3C_2H^- \rightarrow Co_2PtC_2H^- + Co$
$Co_4C_2H^- \rightarrow Co_2C_2H^- + Co_2$

since the dissociation energies of *these reactions* are the least values in Table 2 while the least favorable reactions are

$Co_2Pt_2C_2H^- \rightarrow Co_2C_2H^- + Pt_2$
$Co_3PtC_2H^- \rightarrow Co_3C_2H^- + Pt$

Table 2 The dissociation channels of selected anionic Co_xPt_y-ethynyl clusters

$[Co_xPt_yC_2H]^-$	Dissociation Channel	E_{dis} (eV)
$[Co_3C_2H]^-$	$Co_2C_2H^-$ + Co	2.44
$[Co_2PtC_2H]^-$	$Co_2C_2H^-$ + Pt	4.97
$[CoPt_2C_2H]^-$	$CoPtC_2H^-$ + Pt	3.96
$[Pt_3C_2H]^-$	$Pt_2C_2H^-$ + Pt	4.07
$[Co_4C_2H]^-$	$Co_2C_2H^-$ + Co_2	2.68
$[Co_4C_2H]^-$	$Co_3C_2H^-$ + Co	2.88
$[Co_3PtC_2H]^-$	$Co_3C_2H^-$ + Pt	5.14
$[Co_3C_2H]^-$	$Co_2PtC_2H^-$ + Co	2.61
$[Co_2Pt_2C_2H]^-$	$CoPtC_2H^-$ + CoPt	3.53
$[Co_2Pt_2C_2H]^-$	$Pt_2C_2H^-$ + Co_2	3.99
$[Co_2Pt_2C_2H]^-$	$Co_2C_2H^-$ + Pt_2	5.29

Larger HLGs correspond to better stability. The HLGs are presented in Table 1. HLGs and VDEs of $[Co_xPt_yC_2H]^{-1}$ species are given in Figure 6. $[Co_3C_2H]^{-1}$ has the lowest HLG with the value 0.03 eV in the given study. According to the Table 1, $[Pt_3C_2H]^{-1}$ cluster possesses high chemical stability due to their large HLGs (1.05 eV).

VDE is expressed as the energy difference between neutral and ionic clusters at optimized geometry of the anion clusters. The VDE values in Table 1 are in an agreement with the experimental and theoretical results. The dip is, see Figure 5, seen at $[Co_2C_2H]^{-1}$ (1.25 eV).

We have calculated the vibrational frequencies of all the species, which is given in Table 1 to distinguish transition state isomers.

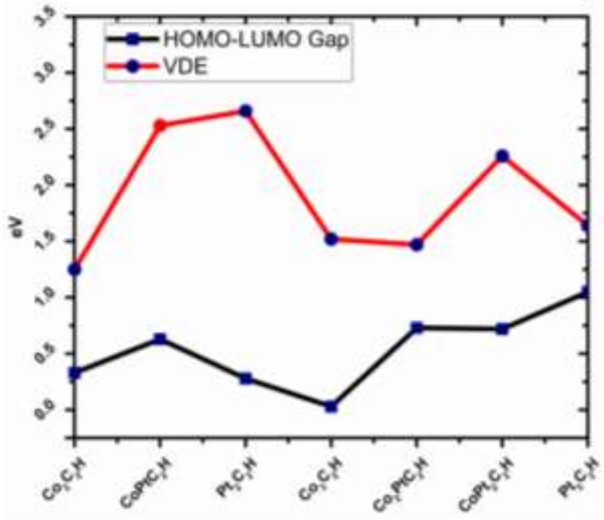

Figure 4 The HOMO-LUMO gaps and VDEs of $[Co_xPt_yC_2H]^-$

4. CONCLUSIONS

In summary, we have investigated the adsorption of ethynyl anion(C_2H^-) to CoPt NPs using density functional theory calculations. For Co_xPt_y-ethynyl subnanoalloy organic structures ($1 \leq x+y \leq 2$) having low symmetric properties, we have found that Pt content leads to increase in BEs. According to the second finite energies calculations, The species $[Co_2PtC_2H]^-$ is found to be more stable structure when comparing their neighboring. The lowest and highest vibrational frequency calculations will guide future spectroscopic experiments.

REFERENCES

[1] F. Tournus, N. Blanc, A. Tamion, P. Ohresser, A. Perez, V. Dupuis. XMCD study of CoPt nanoparticles embedded in MgO and amorphous carbon matrices. Journal of Electron Spectroscopy and Related Phenomena 2008; 166: 84-88.

[2] F. Tournus, A. Tamion, N. Blanc, A. Hannour, L. Bardotti, B. Prével, P. Ohresser, E. Bonet, T. Epicier V. Dupuis Physical Review B 2008; 77: 144411.

[3] M.E. Gruner, G. Rollmann, P. Entel, M. Farle. Multiply Twinned Morphologies of FePt and CoPt Nanoparticles. Physical Review Letters 2008; 100: 087203.

[4] B.H. An, J.H. Wu, H.L. Liu, S.P. Ko, J.S. Ju, Y.K. Kim. CoPt nanoparticles by a modified polyol process. Colloids and Surfaces A: Physicochemical and Engineering Aspects 2008; 313-314: 250-253.

[5] G. Rossi, R. Ferrando, C. Mottet. Structure and chemical ordering in CoPt nanoalloys. Faraday Discussions 2008; 138: 193-210.

[6] P. Moskovkin, M. Hou. Metropolis Monte Carlo predictions of free Co-Pt nanoclusters. Journal of Alloys and Compounds 2007; 434-435: 550-554.

[7] J.K. J.H. Kim, N. Oh, Y-H. Kim, C.K. Kim, C.S. Yoon, S. Jin. Monolayer CoPt magnetic nanoparticle array using multiple thin film depositions. Applied Physics Letters 2007; 90: 023117.

[8] Yuan, Jinyun, Hong-Guang Xu, Zeng-Guang Zhang, Yuan Feng, Weijun Zheng. Adsorption of C_2H Radical on Cobalt Clusters: Anion Photoelectron Spectroscopy and Density Functional Calculations. The Journal of Physical Chemistry 2010; *A*115.2: 182-186.

[9] M.N. Dave, M.L. Wears, J. Michael, C. Desmond. Fabrication and characterization of nano-particulate PtCo media for ultra-high density perpendicular magnetic recording. Nanotechnology 2007; 18: 205301.

[10] L. Favre, V. Dupuis, E. Bernstein, P. Mélinon, A. Pérez, S. Stanescu, T. Epicier, J.P. Simon, D. Babonneau, J.M. Tonnerre, J.L. Hodeau. Physical Review B 2006; 74: 014439.

[11] A. Hannour, L. Bardotti, B. Prével, E. Bernstein, P. Mélinon, A. Perez, J. Gierak, E. Bourhis, D. Mailly. 2D arrays of CoPt nanocluster assemblies. Surface Science 2005; 594: 1-11.

[12] S. Rohart, C. Raufast, L. Favre, E. Bernstein, E. Bonet, V. Dupuis. Magnetic anisotropy of CoxPt1−x clusters embedded in a matrix: Influences of the cluster chemical composition and the matrix nature. Physical Review B 2006; 74: 104408.

[13] T. Seto, K. Koga, H. Akinaga, F. Takano, T. Orii, M. Hirasawa. Laser ablation synthesis of monodispersed magnetic alloy nanoparticles. J Nanopart Res 2006; 8: 371-378.

[14] V. Tzitzios, D. Niarchos, M. Gjoka, N. Boukos, D. Petridis. Synthesis and Characterization of 3D CoPt Nanostructures. Journal of the American Chemical Society 2005; 127: 13756-13757.

[15] M. Mizuno, Y. Sasaki, M. Inoue, C.N. Chinnasamy, B. Jeyadevan, D. Hasegawa, T. Ogawa, M. Takahashi, K. Tohji, K. Sato, S. Hisano. Structural and magnetic properties of monolayer film of CoPt nanoparticles synthesized by polyol process. Journal of Applied Physics 2005; 97: 10J301

[16] L. Castaldi, K. Giannakopoulos, A. Travlos, D. Niarchos, S. Boukari, E. Beaurepaire. CoPt nanoparticles deposited by electron beam evaporation. Journal of Magnetism and Magnetic Materials 2005; 290-291 PART 1: 544-546.

[17] T. Vassilios, N. Dimitrios, M. Gjoka, J. Fidler, P. Dimitrios. Synthesis of CoPt nanoparticles by a modified polyol method: characterization and magnetic properties. Nanotechnology 2005; 16: 287.

[18] Y.-H.X. Jiao-Ming Qiu, Jack, H. Judy, Jian-Ping,Wang, J. P. Nanocluster deposition for high density magnetic recording tape media. Journal of applied physics 2005; 97: 10P704.

[19] Y. Wang, H. Yang. Synthesis of CoPt Nanorods in Ionic Liquids. Journal of the American Chemical Society 2005; 127: 5316-5317.

[20] X. Sun, Z.Y. Jia, Y.H. Huang, J.W. Harrell, D.E. Nikles, K. Sun, L.M. Wang. Synthesis and magnetic properties of CoPt nanoparticles. Journal of Applied Physics 2004; 95: 6747-6749.

[21] C.N. Chinnasamy, B. Jeyadevan, K. Shinoda, K. Tohji. Polyol-process-derived CoPt nanoparticles: Structural and magnetic properties. Journal of Applied Physics 2003; 93: 7583-7585.

[22] H.R. Wang, C.X. Huang, H. Jiang, J.J. Li, J.L. Xu, G.Y. Zhu, B. Yang, X.J. Jiang, G.S. Li. Direct proinflammatory effect of C-reactive protein on human monocytes isolated from patients with acute coronary syndrome and statins intervention. Chinese Pharmacological Bulletin 2004; 20: 1279-1283.

[23] M. Yu, Y. Liu, D.J. Sellmyer. Nanostructure and magnetic properties of composite CoPt:C films for extremely high-density recording. Journal of Applied Physics 87 6959-6961.

[24] Y. Sui, L. Yue, R. Skomski, X.Z. Li, J. Zhou, D.J. Sellmyer. CoPt hard magnetic nanoparticle films synthesized by high temperature chemical reduction. Journal of Applied Physics 2003; 93: 7571-7573.

[25] Y. Xu, Z.G. Sun, Y. Qiang, D.J. Sellmyer. Preparation and magnetic properties of CoPt and CoPt:Ag nanocluster films. Journal of Magnetism and Magnetic Materials 2003; 266: 164-170.

[26] A.C.C. Yu, M. Mizuno, Y. Sasaki, H. Kondo, K. Hiraga. Structural characteristics and magnetic properties of chemically synthesized CoPt nanoparticles. Applied Physics Letters 2002; 81: 3768-3770.

[27] E.V. Shevchenko, D.V. Talapin, A.L. Rogach, A. Kornowski, M. Haase, H. Weller. Colloidal Synthesis and Self-Assembly of CoPt3 Nanocrystals. Journal of the American Chemical Society 2002; 124: 11480-11485.

[28] T.O. Ely, C. Pan, C. Amiens, B. Chaudret, F. Dassenoy, P. Lecante, M.J. Casanove, A. Mosset, M. Respaud, J.M. Broto. Nanoscale Bimetallic CoxPt1-x Particles Dispersed in Polyvinylpyrrolidone;: Synthesis from Organometallic Precursors and Characterization. The Journal of Physical Chemistry B, 2000; 104: 695-702.

[29] Z. Zhang, D.A. Blom, Z. Gai, J.R. Thompson, J. Shen, S. Dai. High-Yield Solvothermal Formation of Magnetic CoPt Alloy Nanowires. Journal of the American Chemical Society 2003; 125: 7528-7529.

[30] D.J. Sellmyer, M. Yu, R.D. Kirby. Nanostructured magnetic films for extremely high density recording. Nanostructured Materials 1999; 12: 1021-1026.

[31] S. Blundell, D. Thouless. Magnetism in condensed matter. American Journal of Physics 2003; 71: 94-95.

[32] W.-F. Huang, Q. Zhang, D.-F. Zhang, J. Zhou, C. Si, L. Guo, W.-S. Chu, Z.-Y. Wu. Investigation of structural and magnetic properties of CoPt/CoAu bimetallic nanochains by x-ray absorption spectroscopy. The Journal of Physical Chemistry C 2013; 117:6872-6879.

[33] M. Valiev, E.J. Bylaska, N. Govind, K. Kowalski, T.P. Straatsma, H.J. Van Dam, D. Wang, J. Nieplocha, E. Apra, T.L. Windus. NWChem: a comprehensive and scalable open-source solution for large scale molecular simulations. Computer Physics Communications 2010; 181: 1477-1489.

[34] M.M. Hurley, L.F. Pacios, P.A. Christiansen, R.B. Ross, W.C. Ermler. Abinitio relativistic effective potentials with spin- orbit operators. II. K through Kr. The Journal of Chemical Physics 1986; 84: 6840-6853.

[35] A.D. Becke. Density-functional exchange-energy approximation with correct asymptotic behavior. Physical Review A 1988; 38: 3098-3100.

[36] C. Lee, W. Yang, R.G. Parr. Development of the Colle-Salvetti correlation-energy formula into a functional of the electron density. Physical Review B 1988; 37: 785.

[37] J.A. Dean. Properties of atoms, radicals, and bonds. Lange's Handbook of Chemistry, 1999; 4.

[38] H. Zhou, H. Tamura, S. Takami, M. Kubo, R. Belosloudov, N. Zhanpeisov. A. Miyamoto, Periodic density functional study on adsorption properties of organic molecules on clean Al (111) surface. Applied Surface Science 2000; 158: 38-42.

[39] A. Sebetci. Cobalt clusters and their anions. Chemical Physics 2008; 354: 196-201.

[40] Q.M. Ma, Z. Xie, J. Wang, Y. Liu, Y.C. Li. Structures, stabilities and magnetic properties of small Co clusters. Physics Letters, Section A: General, Atomic and Solid State Physics 2006; 358: 289-296.

[41] M. Castro, C. Jamorski, D.R. Salahub. Structure, bonding, and magnetism of small Fen, Con, and Nin clusters, $n \leq 5$. Chemical Physics Letters 1997; 271: 133-142.

[42] S. Datta, M. Kabir, S. Ganguly, B. Sanyal, T. Saha-Dasgupta, A. Mookerjee. Structure, bonding, and magnetism of cobalt clusters from first-principles calculations. Physical Review B 2007; 76: 014429.

[43] C. Jamorski, A. Martinez, M. Castro, D.R. Salahub. Structure and properties of cobalt clusters up to the tetramer: A density-functional study. Physical Review B - Condensed Matter and Materials Physics 1997; 55: 10905-10921.

[44] H. Yoshida, A. Terasaki, K. Kobayashi, M. Tsukada, T. Kondow. Spin- polarized electronic structure of cobalt cluster anions studied by photoelectron spectroscopy. The Journal of Chemical Physics 1995; 102: 5960-5965.